

Journal Pre-proof

Suppression of abnormal α -synuclein expression by activation of BDNF transcription ameliorates Parkinson's disease-like pathology

Qianqian Cao, Shilin Luo, Wei Yao, Youge Qu, Nanbu Wang, Jian Hong, Shigeo Murayama, Zhentao Zhang, Jiayu Chen, Kenji Hashimoto, Qi Qi, Ji-chun Zhang

PII: S2162-2531(22)00150-0

DOI: <https://doi.org/10.1016/j.omtn.2022.05.037>

Reference: OMTN 1629

To appear in: *Molecular Therapy: Nucleic Acid*

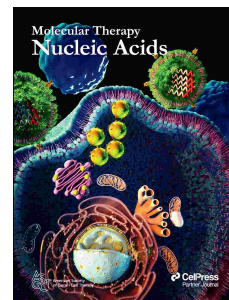
Received Date: 1 April 2022

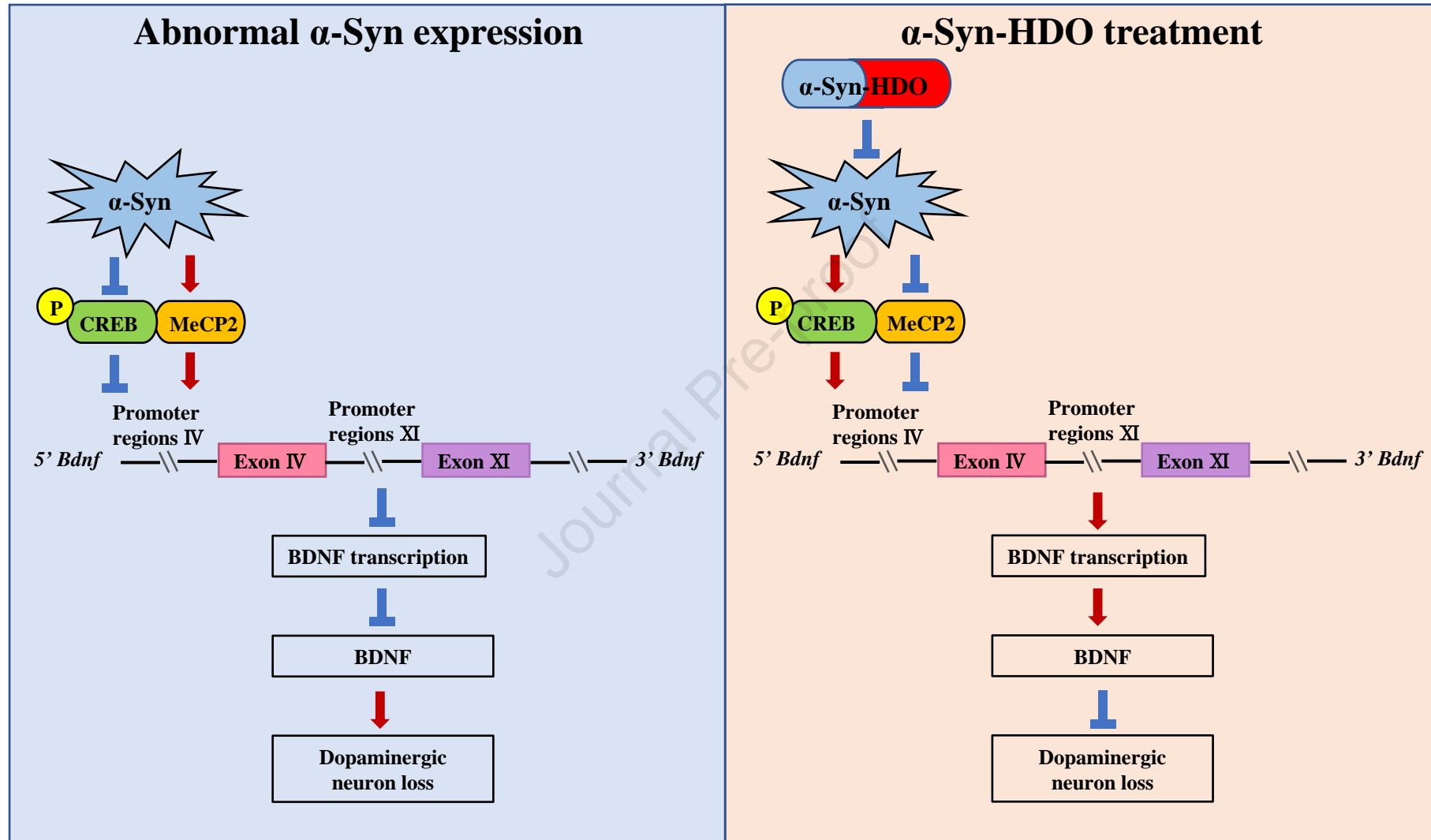
Accepted Date: 26 May 2022

Please cite this article as: Cao Q, Luo S, Yao W, Qu Y, Wang N, Hong J, Murayama S, Zhang Z, Chen J, Hashimoto K, Qi Q, Zhang J-c, Suppression of abnormal α -synuclein expression by activation of BDNF transcription ameliorates Parkinson's disease-like pathology, *Molecular Therapy: Nucleic Acid* (2022), doi: <https://doi.org/10.1016/j.omtn.2022.05.037>.

This is a PDF file of an article that has undergone enhancements after acceptance, such as the addition of a cover page and metadata, and formatting for readability, but it is not yet the definitive version of record. This version will undergo additional copyediting, typesetting and review before it is published in its final form, but we are providing this version to give early visibility of the article. Please note that, during the production process, errors may be discovered which could affect the content, and all legal disclaimers that apply to the journal pertain.

© 2022 The Author(s).





33 **Abstract**

34 Parkinson's disease (PD) is characterized by the formation of Lewy bodies (LBs) in the
35 brain. LBs are mainly composed of phosphorylated and aggregated α -synuclein (α -Syn).
36 Thus, strategies to reduce the expression of α -Syn offer promising therapeutic avenues
37 for PD. DNA/RNA heteroduplex oligonucleotides (HDOs) are a novel technology for
38 gene silencing. Using an α -Syn-HDO that specifically targets α -Syn, we examined
39 whether α -Syn-HDO attenuates pathological changes in the brain of mouse models of
40 PD. Overexpression of α -Syn induced dopaminergic neuron degeneration through
41 inhibition of AMP-responsive-element-binding protein (CREB) and activation of
42 methyl CpG binding protein 2 (MeCP2), resulting in brain-derived neurotrophic factor
43 (BDNF) downregulation. α -Syn-HDO exerted a more potent silencing effect on α -Syn
44 than α -Syn-antisense oligonucleotides (ASOs). α -Syn-HDO attenuated abnormal α -Syn
45 expression and ameliorated dopaminergic neuron degeneration via BDNF upregulation
46 by activation of CREB and inhibition of MeCP2. These findings demonstrated that
47 inhibition of α -Syn by α -Syn-HDO protected against dopaminergic neuron
48 degeneration via activation of BDNF transcription. Therefore, α -Syn-HDO may serve
49 as a new therapeutic agent for PD.

50

51 INTRODUCTION

52 Parkinson's disease (PD), the second most prevalent age-related neurodegenerative
53 disease, is characterized by progressive selective loss of dopaminergic neurons in the
54 substantia nigra pars compacta (SNc) with the concomitant loss of nigrostriatal
55 dopaminergic termini and the resulting motor symptoms ¹. Both genetic and
56 environmental factors play a key role in the etiology of PD ². However, most PD occurs
57 sporadically with unknown disease etiology, and approximately 5%–10% of PD cases
58 are caused by genetic abnormalities ². Both sporadic and familial PD have the same
59 pathological hallmarks as follows: dopaminergic neuron degeneration in the SNc; and
60 the presence of intraneuronal proteinaceous cytoplasmic inclusions, known as Lewy
61 bodies (LBs), in the remaining dopaminergic neurons ^{3,4}. Alpha-synuclein (α -Syn) is
62 the main component of LBs, and its aggregation is believed to be the major step in the
63 pathogenesis of PD ⁵. Mutation or multiplication of α -Syn has been identified as the
64 pathogenesis of both sporadic and familial PD ⁶⁻⁸. Soluble monomers, toxic oligomers,
65 and insoluble fibrils of α -Syn have been detected in the brains of patients with PD ⁹.
66 Several mutations in the gene that encodes α -Syn (*SNCA*), such as A53T, A30P, E46K,
67 H50Q, G51D, and A53E, cause autosomal-dominant PD ¹⁰. Moreover, phosphorylation
68 of α -Syn at the Ser129 site promotes the formation of pathogenic α -Syn aggregates,
69 which is one of the most crucial posttranslational modifications ¹¹. Based on the above
70 findings, downregulation of α -Syn offers a promising therapeutic avenue preventing
71 the progression of PD.

72 Brain-derived neurotrophic factor (BDNF) is a member of the neurotrophin (NT)
73 family ¹²⁻¹⁵. BDNF colocalizes with dopaminergic neurons in the SNc, promoting
74 dopaminergic neuron survival ^{16,17}. Clinical research has revealed that BDNF levels are
75 decreased in PD patients, suggesting that reduced levels of BDNF may be involved in
76 the pathogenesis of PD ^{12, 18}. BDNF transcription is regulated by cyclic AMP-
77 responsive-element-binding protein (CREB) and methyl CpG binding protein 2
78 (MeCP2) ^{19, 20}. CREB is a transcriptional activator, and MeCP2 is a transcriptional
79 repressor of BDNF ^{19,20}. It has been shown that overexpression of α -Syn reduces BDNF
80 expression ²¹. However, the mechanisms by which α -Syn reduce BDNF expression,
81 resulting in PD pathology, have not been defined.

82 In the present study, with *in vitro* and *in vivo* systems, we provide the evidence
83 that overexpression of α -Syn induces dopaminergic neuron degeneration via BDNF
84 downregulation by inhibition of CREB and activation of MeCP2. DNA/RNA
85 heteroduplex oligonucleotides (HDOs) are a newly developed technology for gene
86 silencing²²⁻²⁴. Compared to the parent single-stranded gapmer antisense
87 oligonucleotides (ASOs), a DNA/locked nucleotide acid gapmer duplex with an α -
88 tocopherol-conjugated complementary RNA is significantly more potent in reducing
89 the expression of the targeted mRNA with fewer side effects^{22, 23}. We therefore
90 designed an α -Syn-HDO that specifically targets α -Syn. α -Syn-HDO exerted a more
91 potent silencing effect on α -Syn than α -Syn-ASO. α -Syn-HDO attenuated abnormal α -
92 Syn expression, activated BDNF transcription, and ameliorated dopaminergic neuron
93 degeneration. These findings suggested that abnormal α -Syn expression induces
94 dopaminergic neuron degeneration via inhibition of BDNF transcription, which is
95 alleviated by attenuating abnormal α -Syn expression.

96

97 RESULTS

98 **Overexpression of α -Syn inhibits BDNF expression via inhibition of CREB and** 99 **activation of MeCP2**

100 BDNF plays an important role in neuronal survival in the dopaminergic neurons, and
101 the level of BDNF is reduced in the SNc of PD patients¹⁸. Here, we investigated
102 whether overexpression of α -Syn inhibits BDNF expression via inhibition of CREB
103 and activation of MeCP2. SH-SY5Y cells were transfected with GFP- α -Syn and lysed
104 for western blot analysis. Overexpression of α -Syn decreased the ratio of p-
105 CREB/CREB and BDNF levels; however, it increased MeCP2 expression (**Figure 1A**).
106 These findings suggest that α -Syn causes inhibition of CREB and activation of MeCP2
107 expression, resulting in BDNF downregulation.

108 Next, we injected AAV9-hSyn-human SNCA virus into the SNc of WT mice.
109 Subsequently, we extracted proteins from the SNc for western blot analysis. Injection
110 of AAV9-hSyn-human SNCA decreased the ratio of p-CREB/CREB and BDNF levels;

111 however, it increased MeCP2 expression (**Figure 1B**).

112 Dementia with Lewy bodies (DLB) is pathologically characterized by α -Syn, and
113 phosphorylated α -Syn aggregates in the brain²⁵. Deposition of α -Syn has been shown
114 in multiple brain regions of PD and DLB patients^{25, 26}. Therefore, postmortem brain
115 samples from patients with DLB were used. We measured the protein expression of p-
116 CREB/CREB, BDNF, and MeCP2 in the striatum from DLB patients and age-matched
117 control subjects. The ratio of p-CREB/CREB and the levels of BDNF were significantly
118 lower in patients with DLB than in controls. Furthermore, the levels of MeCP2 in
119 patients with DLB were significantly higher than those of controls (**Figure 1C**).
120 Interestingly, there was a positive correlation between BDNF levels and p-
121 CREB/CREB ratio in the striatum from DLB patients (**Figure 1C**). Furthermore, there
122 was a negative correlation between BDNF levels and MeCP2 levels in the striatum from
123 DLB patients (**Figure 1C**). Collectively, these findings indicated that overexpression
124 of α -Syn causes inhibition of CREB and activation of MeCP2, resulting in BDNF
125 downregulation.

126 **Silencing α -Syn expression activates BDNF transcription**

127 In the present study, we designed an α -Syn-HDO that harbors locked nucleic acids
128 (LNAs) at each end flanking the central base of DNA and 2'-O-methyl at each end
129 flanking the central base of cRNA with conjugated α -tocopherol. The α -Syn-HDO was
130 also tagged with or without FAM labels for tracing (**Figure 2A**). FAM- α -Syn-HDO
131 was absorbed in SH-SY5Y cells in a time-dependent manner (**Figure 2B**). Western blot
132 analysis showed that α -Syn-HDO decreased α -Syn and MeCP2 expression in a dose-
133 dependent manner (**Figure 2C**), while α -Syn-HDO increased the ratio of p-
134 CREB/CREB and BDNF expression in a dose-dependent manner (**Figure 2C**).
135 Moreover, compared to α -Syn-ASO (200 nM), α -Syn-HDO (200 nM) exerted a more
136 potent silencing effect on α -Syn at both the mRNA and protein levels (**Figure S1A** and
137 **B**). In addition, the IC₅₀ of α -Syn-HDO (64.06 nM) is more potent than α -Syn-ASO
138 (99.81 nM) (**Figure S1C** and **D**). The scrambled α -Syn-HDO did not show any

139 silencing effect for Δ -Syn (**Figure S2A and B**). The results suggest that Δ -Syn-HDO
140 effectively silences Δ -Syn expression. Based on the *in vitro* results, we examined the
141 silencing effects of Δ -Syn-HDO for Δ -Syn *in vivo*. Mice were subjected to
142 intracerebroventricular (ICV) injection of Δ -Syn-HDO (200 nM/2 μ l/week, total 4
143 times). Western blot analysis showed that Δ -Syn-HDO significantly decreased Δ -Syn
144 expression in the SNc of WT mice (**Figure S3A**). In addition, we compared the
145 silencing effects of Δ -Syn-ASO and Δ -Syn-HDO *in vivo*. ICV injection of Δ -Syn-ASO
146 or Δ -Syn-HDO (200 nM/2 μ l/week, total 4 times) decreased Δ -Syn and MeCP2
147 expression (**Figure S3B**), while Δ -Syn-ASO or Δ -Syn-HDO increased the p-
148 CREB/CREB ratio and BDNF expression in the SNc of WT mice (**Figure S3B**).
149 Importantly, Δ -Syn-HDO was more potent than Δ -Syn-ASO. These results suggest that
150 Δ -Syn-HDO is associated with the activation of BDNF transcription by silencing Δ -Syn
151 expression.

152 To further elucidate the action of Δ -Syn-HDO in stimulating BDNF transcription,
153 we performed luciferase reporter, chromatin immunoprecipitation (ChIP)-PCR, and
154 quantitative real-time PCR (qPCR) assays. The data showed that Δ -Syn-HDO activated
155 the *Bdnf* exon IV promoter, which was blocked by CREB knockdown (**Figure 2D and**
156 **E**). In addition, mutation in the CREB-binding motif completely abolished promoter
157 activity (**Figure 2E**). In addition, ChIP-PCR analysis of genomic DNA
158 immunoprecipitated with the p-CREB antibody demonstrated that Δ -Syn-HDO induced
159 the interaction between p-CREB and the *Bdnf* exon IV promoter (**Figure 2F**). Moreover,
160 Δ -Syn-HDO enhanced the *Bdnf* mRNA levels (**Figure 2G**). Collectively, these data
161 demonstrated that Δ -Syn-HDO activates CREB, resulting in BDNF transcription.

162 **Δ -Syn-HDO is associated with activation of CREB and inhibition of MeCP2,**
163 **resulting in BDNF upregulation in Δ -Syn-treated SH-SY5Y cells**

164 Overexpression of Δ -Syn leads to inhibition of CREB and activation of MeCP2, thereby
165 causing BDNF downregulation. Hence, we further explored whether Δ -Syn-HDO
166 associates with BDNF upregulation in Δ -Syn-treated SH-SY5Y cells. To address this

167 hypothesis, SH-SY5Y cells were transfected with GFP- α -Syn or GST- α -Syn.
168 Overexpression of α -Syn significantly decreased the ratio of p-CREB/CREB and
169 BDNF levels but it increased MeCP2 expression (**Figure 3A**). α -Syn-HDO reversed
170 the effects of α -Syn overexpression in GFP- α -Syn-transfected SH-SY5Y cells (**Figure**
171 **3A**). Immunofluorescence staining revealed that overexpression of α -Syn caused the
172 redistribution of p-CREB and MeCP2 in the nucleus of SH-SY5Y cells. α -Syn induced
173 MeCP2 nuclear localization and more punctate p-CREB in the nucleus, and this
174 redistribution was reversed by α -Syn-HDO (**Figure 3B**). These data demonstrated that
175 α -Syn-HDO can attenuate BDNF downregulation in α -Syn-treated SH-SY5Y cells.

176 **α -Syn-HDO attenuates dopaminergic neuron degeneration in an α -Syn-induced** 177 **PD mouse model**

178 To examine potential therapeutic efficacy of α -Syn-HDO, we investigated whether α -
179 Syn-HDO attenuates dopaminergic neuron degeneration via activation of BDNF
180 transcription in AAV9-hSyn-human SNCA-treated mice. First, AAV9-hSyn-human
181 SNCA was injected into the SNc of wild-type (WT) mice to construct a PD mouse
182 model (**Figure 4A**). Subsequently, mice were subjected to intracerebroventricular (ICV)
183 injection of FAM- α -Syn-HDO or α -Syn-HDO (200 nM/2 μ l/week, total 4 times)
184 (**Figure 4A**). Following confirmation of the distribution of FAM- α -Syn-HDO in the
185 mouse brains (**Figure 4B**), behavioral tests showed that α -Syn-HDO significantly
186 prolonged the duration of AAV9-hSyn-human SNCA-treated mice on the rotarod test
187 compared to those of the vehicle group (**Figure 4C**). Immunofluorescence staining
188 demonstrated that AAV9-hSyn-human SNCA administration significantly decreased
189 TH immunoreactivity but increased IBA1 and GFAP immunoreactivity in the SNc, and
190 these changes were reversed by α -Syn-HDO (**Figure 4D** and **Figure S4**). Using western
191 blot analysis, we found that AAV9-hSyn-human SNCA significantly downregulated
192 TH expression but increased α -Syn levels in the SNc, which was reversed by α -Syn-
193 HDO (**Figure 4E**). Collectively, these data suggest that α -Syn-HDO attenuates
194 dopaminergic neuron degeneration and ameliorates PD-like pathology in AAV9-hSyn-

195 human SNCA-treated mice.

196 To further validate the connections of therapeutic activity and the above regulation
197 of α -Syn-HDO *in vivo*, we examined signaling in the SNc of AAV9-hSyn-human
198 SNCA-treated mice. ChIP-PCR results showed that p-CREB partially dissociated from
199 the *Bdnf* exon IV promoter, which was reversed by α -Syn-HDO (**Figure 4F**). Next, we
200 examined the ratio of p-CREB/CREB and the protein levels of BDNF and MeCP2 in
201 the SNc of AAV9-hSyn-human SNCA-treated mice. The data showed that the p-
202 CREB/CREB ratio and BDNF expression were decreased and that MeCP2 expression
203 was increased. Interestingly, α -Syn-HDO increased the ratio of p-CREB/CREB and
204 decreased MeCP2 expression, leading to BDNF upregulation (**Figure 4G**). Therefore,
205 these findings indicated that α -Syn-HDO can produce neuroprotective effects by
206 promoting BDNF expression in AAV9-hSyn-human SNCA-treated mice *via* activation
207 of CREB and inhibition of MeCP2.

208

209 **α -Syn-HDO attenuates dopaminergic neuron degeneration in MPTP-treated α - 210 Syn-A53T mice**

211 MPTP is the best characterized toxin that causes PD pathology, and injection of MPTP
212 accelerates PD pathology in SNCA mice *in vivo*^{12, 27}. Hence, we further examined the
213 neuroprotective effect of α -Syn-HDO in MPTP-treated α -Syn-A53T mice. ICV
214 injection of α -Syn-HDO significantly increased the duration of MPTP-treated α -Syn-
215 A53T mice on the rotarod test compared to the vehicle group (**Figure 5A and B**).
216 Immunofluorescence staining indicated that α -Syn-HDO significantly increased TH
217 immunoreactivity but decreased IBA1 and GFAP immunoreactivity in the SNc of
218 MPTP-treated α -Syn-A53T mice compared to the vehicle group (**Figure 5C and Figure**
219 **S5**). Western blot analysis showed that α -Syn-HDO increased TH immunoreactivity
220 but decreased α -Syn protein expression in the SNc of MPTP-treated α -Syn-A53T mice
221 (**Figure 5D**). These data demonstrated that α -Syn-HDO ameliorates PD-like pathology
222 in MPTP-treated α -Syn-A53T mice.

223 ChIP-PCR results showed that p-CREB partially dissociated from the *Bdnf* exon

224 IV promoter in MPTP-treated Δ -Syn-A53T mice, which was reversed by Δ -Syn-HDO
225 (**Figure 5E**). We also found that the p-CREB/CREB ratio and BDNF expression were
226 decreased and that MeCP2 expression was increased, and these changes in MPTP-
227 treated Δ -Syn-A53T mice were reversed by Δ -Syn-HDO (**Figure 5F**). Therefore, these
228 findings suggested that Δ -Syn-HDO can produce neuroprotective effects by promoting
229 BDNF expression in MPTP-treated Δ -Syn-A53T mice.

230 **Δ -Syn-HDO blocks Δ -Syn pathology *in vitro* and *in vivo***

231 To determine whether the reduction of Δ -Syn expression by Δ -Syn-HDO ameliorates
232 Δ -Syn aggregation, we assessed the effects of Δ -Syn-HDO on the aggregation and
233 phosphorylation of Δ -Syn in Δ -Syn-preformed fibrils (PFFs). We detected the
234 aggregation of Δ -Syn in HEK293- Δ -Syn cells. After treatment with PFFs for 24 hours,
235 YFP- Δ -Syn started to aggregate into small fluorescence spots located in the intracellular
236 space, and this effect was abolished by Δ -Syn-HDO treatment (**Figure S6A and S6B**).
237 Western blot analysis showed that the PFFs induced phosphorylation of Δ -Syn at S129
238 (p-S129), which was attenuated by Δ -Syn-HDO (**Figure S6C**). PFFs were injected into
239 the SNc of Δ -Syn-A53T mice *in vivo*, which led to the cell-to-cell transmission of
240 pathologic Δ -Syn and PD-like Lewy pathology in the SNc (**Figure 6A**). Treatment with
241 Δ -Syn-HDO significantly attenuated the PFFs-induced Lewy pathology in the SNc
242 (**Figure 6A**). In behavioral tests, Δ -Syn-HDO prolonged the duration of PFFs-treated
243 Δ -Syn-A53T mice on the rotarod test compared to the vehicle group (**Figure 6B**).
244 Immunofluorescence staining demonstrated that Δ -Syn-HDO significantly increased
245 TH immunoreactivity but decreased IBA1 and GFAP immunoreactivity in the SNc of
246 PFFs-treated Δ -Syn-A53T mice (**Figure 6C and Figure S7A and S7B**). Western blot
247 assays showed that Δ -Syn-HDO treatment significantly ameliorated the decreased
248 expression of TH and increased expression of p-S129 and Δ -Syn in the SNc of PFFs-
249 treated Δ -Syn-A53T mice (**Figure 6D**). These results indicated that Δ -Syn-HDO could
250 ameliorate the phosphorylation and aggregation of Δ -Syn, resulting in attenuation of
251 PD pathology.

252 In addition, ChIP-PCR results showed that p-CREB partially dissociated from the
253 *Bdnf* exon IV promoter in PFFs-treated Δ -Syn-A53T mice, which was reversed by Δ -

254 **Syn-HDO (Figure 6E)**. Western blot results found that the p-CREB/CREB ratio and
255 BDNF expression were decreased and that MeCP2 expression was increased, and these
256 changes were reversed by β -Syn-HDO in PFFs-treated β -Syn-A53T mice (**Figure 6F**).
257 Therefore, these findings indicated that β -Syn-HDO exerts neuroprotective effects by
258 promoting BDNF expression in PFFs-treated β -Syn-A53T mice.

259

260 DISCUSSION

261 In the present study, overexpression of β -Syn induced dopaminergic neuron
262 degeneration via inhibition of CREB and activation of MeCP2, resulting in BDNF
263 downregulation. Silencing abnormal β -Syn expression using β -Syn-HDO activated
264 CREB and inhibited MeCP2, resulting in BDNF upregulation and amelioration of
265 dopaminergic neuron degeneration in PD mouse models. Our results suggest that
266 overexpression of β -Syn inhibits BDNF expression, resulting in PD pathology. Thus,
267 downregulation of abnormal β -Syn expression offers a promising therapeutic avenue
268 preventing the progression of PD.

269 Accumulating studies have shown that BDNF colocalizes with dopaminergic
270 neurons in the SNc and that BDNF promotes dopaminergic neuronal survival^{12, 28, 29}.
271 Reduced levels of BDNF have been demonstrated in the postmortem brains of PD
272 patients^{12, 18, 30}. β -Syn-induced blockade of TrkB neurotrophic activation triggers
273 dopaminergic neuronal death in a PD mouse model¹². In contrast, overexpression of
274 BDNF attenuates 6-OHDA- or MPTP-induced nigrostriatal degeneration, and it
275 improves rotational behavioral deficits by regulating dopaminergic neurotransmission
276^{31, 32}. Therefore, BDNF is integral to both the pathophysiology of PD and the therapeutic
277 mechanisms for PD. In the present study, we found that overexpression of β -Syn
278 inhibited BDNF expression by decreasing the ratio of p-CREB/CREB and increasing
279 MeCP2 expression. In addition, the ratio of p-CREB/CREB and the levels of BDNF
280 were significantly lower in the postmortem brain samples from patients with DLB,
281 whereas the levels of MeCP2 were significantly higher in these samples. Therefore,
282 these data indicated that overexpression of β -Syn inhibits CREB and activates MeCP2,
283 resulting in BDNF downregulation, which plays a role in the pathogenesis of PD.

284 Overexpression of BDNF has been shown to attenuate dopaminergic neuron
285 degeneration^{31,32}. Our data showed that α -Syn-HDO attenuated dopaminergic neuronal
286 degeneration in PD mouse models. Therefore, we examined whether α -Syn-HDO
287 promotes BDNF transcription by inhibiting of abnormal α -Syn expression. *In vitro* data
288 revealed that α -Syn-HDO promoted p-CREB binding with *Bdnf* exon IV promoter,
289 resulting in *Bdnf* mRNA expression. The results indicated that α -Syn-HDO activates
290 BDNF transcription. *In vivo* data suggested that α -Syn-HDO attenuated dopaminergic
291 neuron degeneration in the SNc of PD mouse models, and that α -Syn-HDO attenuated
292 the dissociated effects of the p-CREB binding with *Bdnf* exon IV promoter in the SNc
293 of PD mouse models. In addition, α -Syn-HDO restored the reduction of p-CREB/CREB
294 ratio and increased MeCP2 expression, resulting in BDNF expression through
295 inhibition of abnormal α -Syn expression. Thus, it is likely that α -Syn-HDO might
296 produce neuroprotective effects through inhibition of α -Syn expression in PD mouse
297 models, leading to upregulation of CREB activity and downregulation of MeCP2
298 expression, which activated BDNF transcription. Besides, the abnormal α -Syn
299 promotes the production of reactive oxygen species (ROS) through interaction with
300 complex I of the mitochondrial respiratory chain and interferes with its function³³.
301 Accumulating evidence suggests that the toxic interaction between dopamine (DA), DA
302 metabolites, and abnormal α -Syn might promote an oxidative environment within
303 dopaminergic neurons. Oxidative modification of α -Syn by DA metabolites has been
304 proposed to be responsible for the selective vulnerability to dopaminergic neurons^{34,35}.
305 The oligomeric α -Syn has been suggested to represent the primary toxic species
306 responsible for dopaminergic neurotoxicity³⁴. These evidences suggest that abnormal
307 α -Syn may cause neurodegeneration in other pathways excluding BDNF pathway.
308 Suppression of abnormal α -Syn by α -Syn-HDO may prevent neurodegeneration
309 beyond the CREB-BDNF signaling pathway. Therefore, it is of interest to investigate
310 the role of other signaling pathways on the neuroprotective effects of α -Syn-HDO. In
311 addition, altered levels of p-CREB and MeCP2 can affect the regulation of numerous
312 genes. It is, therefore, possible that changes in widespread genes could affect MPTP-
313 induced neurotoxicity, contributing to the effects of α -Syn-HDO in MPTP-treated α -
314 Syn-A53T mice.

315 Chronic neuroinflammation, one of the key pathogenic factors responsible for
316 neurodegenerative disorders, can lead to elevated levels of glia-derived cytokines,
317 which exert neurotoxic effects on vulnerable dopaminergic neurons³⁶⁻³⁸. In the animal
318 models of PD and PD patients, reactive microglia / astrocytes (CD11b / GFAP) were
319 found in the SNc, indicating the possible involvement of gliosis-derived inflammatory
320 processes responsible for PD³⁹. Inhibition of glial activation-derived inflammatory
321 response contributes to the protection of dopaminergic neurons *in vivo* and *in vitro*⁴⁰.
322 In this study, we found that chronic administration of α -Syn-HDO could prevent glial
323 activation and attenuate TH neurons degeneration in the SNc of PD mouse models.
324 Taken together, the present data suggest that the neuroprotective effects of α -Syn-HDO
325 might be partly mediated by inhibiting the activation of glial SNc of PD mouse models
326 although further study is needed.

327 As demonstrated by various genetic and biochemical studies, α -Syn is the major
328 component of LBs and plays a predominant role in the pathogenesis of PD and DLB⁴¹,
329 ⁴². There is extensive phosphorylation of α -Syn at S129 in LBs⁴³. Therefore, the most
330 likely hypothesis is that phosphorylation of α -Syn at Ser129 accelerates the formation
331 of insoluble α -Syn aggregates during the onset of PD⁴⁴. Moreover, exogenous PFFs
332 have been reported to induce the aggregation of endogenous α -Syn^{42, 45}. Using
333 HEK293 cells stably transfected with human α -Syn, we found that α -Syn-HDO
334 decreased the expression, phosphorylation, and aggregation of α -Syn. In addition,
335 dopaminergic neuron degeneration in PFFs-treated α -Syn-A53T mice was attenuated
336 by α -Syn-HDO. These data suggested that α -Syn-HDO reduces α -Syn levels,
337 consequently alleviating α -Syn-induced pathological changes.

338 The present study has some limitations. The previous study has shown that the α -
339 Syn knock out (KO) mice did exhibit abnormalities in synaptic morphology and
340 function, along with fairly subtle behavioral changes^{46, 47}. The α -Syn-HDO is widely
341 distributed throughout the brain by ICV injection. Therefore, the neurotoxic effects and
342 off-target effects of α -Syn-HDO should be further studied, especially in normal mice
343 for long periods of time. Moreover, the striatum includes caudate, putamen and globus
344 pallid, which is innervated from multiple brain regions, so any changes observed cannot
345 exclusively be attributed to the nigrostriatal pathway. In addition, the striatum is also
346 only the terminal region of the nigrostriatal system and changes in transcription factors

347 may not only reflect what is happening in the soma of the neurons in the nigra. Future
348 study using post-mortem samples of nigra is needed. Finally, it has shown that
349 overexpression of human- α -Syn under the Thy1 regulatory element promotes
350 expression of human- α -Syn in multiple neuronal subpopulations. Intriguingly, this did
351 not include TH-positive dopaminergic neurons which do not degenerate in these mice⁴⁸,
352 inconsistent with our results. The difference may be due to different promoters for
353 human- α -Syn. Future detailed studies are necessary to explore these differences.

354 In conclusions, the current study suggests that overexpression of α -Syn induces
355 dopaminergic neurons degeneration through inhibition of BDNF transcription, and that
356 the novel nucleic acid agent α -Syn-HDO can attenuate dopaminergic neurons
357 degeneration in PD mouse models via activation of BDNF transcription. Therefore, α -
358 Syn-HDO would be a potential new therapeutic agent for PD.

359

360 MATERIALS AND METHODS

361 **Mice and cell lines**

362 Male adult C57BL/6 mice (8 weeks old, 20–25 g) were obtained from Guangdong
363 Experimental Animal Center. Male transgenic mice expressing A53T human α -Syn
364 (12 weeks old, 25–30 g) were obtained from the Jackson Laboratory (gift from Dr.
365 Zhentao Zhang). The animals were housed under controlled temperature and kept in a
366 12-h light/dark cycle with *ad libitum* access to food and water. The animal protocol was
367 approved by the Jinan University Institutional Animal Care and Use Committee, and
368 all experiments were performed following the Guide for Animal Experimentation of
369 Jinan University. HEK293T cells, SH-SY5Y cells, and HEK293T cells stably
370 expressing YFP-labeled human α -synuclein (HEK293- α -Syn) were cultured in DMEM
371 or DMEM/F-12 (basal media) supplemented with 10% fetal bovine serum (Excell Bio.)
372 and penicillin (100 units/mL)–streptomycin (100 μ g/mL). Cells were cultured at 37 °C
373 in a humidified incubator containing 5% CO₂. HEK293- α -Syn cells were kindly gifted
374 by Prof. Dimond⁴⁹.

375

376 **Materials**

377 MPTP (1-methyl-4-phenyl-1,2,5,6-tetrahydropyridine) was purchased from Yuanye
 378 Bio-Technology (Shanghai, China) and dissolved in 0.9% sterile saline. MPTP
 379 (30 mg/kg) was administered intraperitoneally (i.p.) to mice. The doses of MPTP
 380 selected correspond to those previously reported⁵⁰. The pEGFP- α -Syn and mGST- α -
 381 Syn plasmids were kindly gifted by Dr. Zhentao Zhang (Department of Neurology,
 382 Renmin Hospital of Wuhan University).

383 Antisense oligonucleotides (ASOs) for α -Syn and cRNA were purchased from
 384 TsingKe Biological Technology (Wuhan, China) or Ajinomoto Bio-Pharma (Osaka,
 385 Japan) and solubilized in 0.9% sterile saline before use. For the ion of α -Syn-HDO,
 386 equimolar amounts of DNA and cRNA strands were heated in 0.9% sterile saline at
 387 95 °C for 5 minutes and slowly cooled to room temperature. HDO harbored locked
 388 nucleic acids (LNAs) at each end flanking the central base of DNA with or without a
 389 FAM (6-carboxy-fluorescein) label, and HDO harbored 2'-O-methyl at each end
 390 flanking the central base of cRNA with conjugated α -tocopherol. The sequences of
 391 ASOs and cRNA targeting α -Syn used in our experiments are as follows: ASO- α -Syn,
 392 G(L)⁴C(L)⁴t⁴c⁴c⁴c⁴t⁴c⁴a⁴c⁴t⁴g⁴T(L)⁴C(L)⁴T(L)⁴; cRNA,
 393 a(M)⁴g(M)⁴a(M)⁴caguggaggga⁴g(M)⁴c(M)⁴; where L indicates the locked nucleic
 394 acids; M indicates the 2'-O-methyl modifications; and ^ indicates the phosphorothioate
 395 bond. SH-SY5Y cells were transfected with different doses of α -Syn-HDO for 24 h
 396 using Lipofectamine 3000 (Invitrogen) according to the manufacturer's instructions.
 397 After transfection for 24 h, cells were collected for luciferase reporter, CHIP-PCR,
 398 immunofluorescence staining, qPCR and western blot assays.

399 Full-length human α -Syn was expressed in BL21 (DE3) competent E. coli (Life
 400 Technologies) and purified as previously described⁵¹. The purified recombinant α -Syn
 401 was stored at -80 °C until use. Preformed fibrils (PFFs) were made by diluting
 402 recombinant α -Syn to 5 mg/ml in sterile Dulbecco's PBS (Cellgro, Mediatech; pH
 403 adjusted to 7.0, without Ca²⁺ or Mg²⁺) followed by incubation at 37 °C with constant

404 agitation at 1,000 rpm for 7 days. PFFs were sonicated with a water-bath cup-horn
405 sonicator (Fisher Scientific, USA) at 50% power for 5 minutes before use.

406

407 **Treatment with AAV9-hSyn-human SNCA, PFFs, and α -Syn-HDO**

408 Mice were anesthetized with isoflurane and fixed to a stereotaxic apparatus. AAV9-
409 hSyn-human SNCA (6.58×10^{13} vg / ml, Vigenebio Biosciences, Jinan, China) or PFFs
410 were injected into the substantia nigra (1.2 mm lateral, -4.3 mm ventral, and -3.1 mm
411 from Bregma)¹. Virus (2 μ l) or PFFs (2.5 μ l) were injected into each site using a 10 μ l
412 Hamilton syringe with a fixed needle at a rate of 0.25 μ l/min using a microinjector
413 pump (KDS, Stoelting). The needle remained in place for 5 minutes after the viral
414 suspension or PFFs were completely injected followed by slow removal (over 2
415 minutes). The mice were placed on a heating pad until recovery from anesthesia.

416 α -Syn-HDO was injected into the right lateral ventricle using the following
417 stereotaxic coordinates: 0.8 mm lateral, -2.1 mm ventral, and 0.74 mm from bregma
418 following anesthetization. For multiple injections of α -Syn-HDO over four weeks (α -
419 Syn-HDO: 200 nM/2 μ l/week, total 4 times), a guiding cannula (RWD Life Science,
420 China) was implanted using the coordinates described above. The expected depth was
421 1.3 mm ventrally, and drugs were injected by an injection cannula through a guiding
422 cannula.

423

424 **Rotarod test**

425 For the rotarod test, mice were trained for 3 sequential days on the rotarod. Each daily
426 practice session consisted of placing the subject on the rotarod at a slow rotational
427 speed (5 rpm) for a maximum of 5 min. Mice were given three test trials on the test
428 day. The rotational speed of rotarod was modulated from 0 rpm to a maximum 40
429 rpm. It was gradually increased during the trial at a rate of 0.1 rpm/s. Each trial was
430 started and then sustained for 5 minutes. The trial was stopped when the mouse fell
431 (activating a switch that automatically stopped the timer) or when 5 minutes had

432 elapsed. The residence time on the rotarod was counted using a stopwatch. The results
433 showed the average value of the three trials.

434

435 **qPCR assay**

436 Levels of *-Syn* and *Bdnf* mRNA were examined by quantitative real-time PCR. RNA
437 was extracted using an Eastep® Super Kit (Promega) followed by reverse transcription
438 with GoScript™ Reverse Transcriptase Mix, Oligo (dT) (Promega) to generate cDNA.
439 The real-time PCR assays were performed with the ChamQ™ SYBR® qPCR Master
440 Mix Kit (Vazyme) using the 788BR05175 Real-Time PCR System. The PCR
441 amplification protocol was as follows: 40 cycles of denaturation at 95 °C for 30 seconds,
442 annealing at 55 °C for 30 seconds, and extension for 30 seconds at 72 °C. The primer
443 sequences were as follows: *-Syn* forward, 5' TGACGGGTGTGACAGCAGTAG 3';
444 *-Syn* reverse, 5' CAGTGGCTGCTGCAATG 3'; *Bdnf* forward, 5'
445 TTGTTTTGTGCCGTTTACCA 3'; *Bdnf* reverse, 5'
446 GGTAAGAGAGCCAGCCACTG 3' for mouse sample; *Bdnf* forward, 5'
447 CATCCGAGGACAAGGTGGCTTGG3'; and *Bdnf* reverse, 5'
448 GTCCTCATCCAACAGCTCTTCTATC3' for human sample^{4, 52, 53}. The target genes
449 were analyzed by the 2^{-Ct} method.

450

451 **Western blot analysis**

452 Cell and brain homogenates were lysed in RIPA buffer. Protein concentrations were
453 determined by a Coomassie Brilliant Blue protein assay kit (Bio-Rad). Postmortem
454 brain samples (striatum) from DLB patients and age-matched controls were collected
455 at Tokyo Metropolitan Geriatric Hospital and Institute of Gerontology (Tokyo, Japan).
456 Brain samples were selected using the Brain Bank for Aging Research (BBAR) Lewy
457 bodies rating system⁵⁴. Total protein (20 µg) was separated on 10%-12% sodium
458 dodecyl sulfate-polyacrylamide gels and then transferred to polyvinylidene difluoride
459 (PVDF) membranes. The membranes were blocked with 5% milk at room temperature
460 for 1 hour followed by incubation with primary antibodies at 4 °C for 12 hours.

461 Membranes were then washed three times with TBST and incubated with the
462 corresponding secondary antibody for 1 hour at room temperature. After an additional
463 three washes, targeted proteins were detected using the enhanced chemiluminescence
464 method scanned by the Tanon-5200CE imaging system (Tanon, Shanghai, China). The
465 expression levels of target proteins were normalized to β -actin as a loading control. The
466 following primary antibodies were used: anti-phospho-CREB antibody (1:1000, 9198S)
467 and CREB antibody (1:1000, 9197S) were purchased from Cell Signaling Technology;
468 anti-MeCP2 antibody (1:1000, M6818) was purchased from Sigma; anti-BDNF
469 antibody (1:1000, ab108319), anti-phospho- τ -Syn antibody (1:1000, ab51253), and
470 anti- τ -Syn antibody (1:1000, ab1903) were purchased from Abcam; anti-tyrosine-
471 hydroxylase (TH) antibody (1:1000, GTX10372) was purchased from GTX (GeneTex);
472 and anti- β -actin antibody was purchased from EarthOx. The HRP-conjugated anti-
473 rabbit/mouse IgG antibody was purchased from BIO-RAD.

474

475 **Immunofluorescence staining**

476 Cell or mouse brain sections were preplated on cover glasses and fixed in 4% PFA for
477 10 minutes at room temperature. After treatment, the glasses were washed with PBS 3
478 times and blocked using 3% BSA with 0.3% Triton X-100 for 30 minutes followed by
479 incubation with anti-TH (1:500, GTX10372), anti-IBA1 (1:500, GTX632426), or anti-
480 GFAP (1:500, Affinity, DF6040) primary antibodies for 24 hours at 4 °C. Following
481 washing with PBS, cells were incubated with Alexa Fluor 488/594 anti-mouse/rabbit
482 secondary antibody (1:500) for 2 hours at room temperature in the dark followed by
483 staining with DAPI to visualize the nuclei. Cells were washed with PBS and visualized
484 by a fluorescence microscope (Olympus BX53, Japan).

485

486 **Luciferase reporter assay**

487 HEK293T cells were cotransfected with BDNF exon IV luciferase reporter plasmid
488 together with pRL-TK Renilla luciferase plasmid (Promega) and τ -Syn-HDO, siRNA-
489 CREB, or CREB mutant plasmid. after transfection for 24 hours, cells were collected

490 and analyzed using the dual-luciferase reporter assay kit (Promega) according to the
491 manufacturer's protocol.

492

493 **ChIP-PCR assay**

494 Following treatment with -Syn-HDO, cells or brain samples were analyzed by a ChIP-
495 PCR assay using the SimpleChIP® Enzymatic Chromatin IP Kit (Cell Signaling)
496 according to the manufacturer's protocol. For the ChIP assay, 7.5 µg of p-CREB
497 antibody was added to the sample homogenate, mixed, and incubated overnight at 4 °C.
498 The washing, elution, and reverse cross-linking to free DNA were performed according
499 to the manufacturer's protocol. BDNF exon IV-specific primers were used for
500 amplification of the promoter region using the following primer sequences: forward 5'
501 GGCTTCTGTGTGCGTGAATTTGC 3' and reverse 5'
502 AAAGTGGGTGGGAGTCCACGAG²⁰. The PCR amplicon was separated on a 2%
503 agarose gel after 35 cycles of PCR (denaturation at 95 °C for 30 seconds, annealing at
504 58 °C for 30 seconds, and extension at 72 °C for 30 seconds).

505

506 **Statistical analysis**

507 All data results are expressed as the mean ± standard error of the mean (SEM) and were
508 analyzed using PASW Statistics 20 software (formerly SPSS Statistics, SPSS).
509 Potential differences between the mean values were evaluated using one-way analysis
510 of variance followed by *post hoc* Fisher's least significant difference test or two-way
511 analysis of variance; when appropriate, post hoc comparisons were performed using the
512 unpaired *t*-test. Student's *t*-test was used to compare the differences between two
513 groups unless otherwise specified. Asterisks were used to indicate significance: **P* <
514 0.05, ***P* < 0.01, and ****P* < 0.001. Values > 0.05 were considered not significant (ns).

515

516 **ACKNOWLEDGMENTS**

517 We thankful to Dr. Zhentao Zhang (Department of Neurology, Renmin Hospital of
518 Wuhan University) for providing the A53T mice for us. This work is supported by the
519 National Natural Science Foundation of China (81973341 to QQ, 81822016 and
520 81771382 to ZZ), the Science and Technology Program of Guangzhou (202002030010
521 to QQ), the Fundamental Research Funds for the Central Universities (11620425 to JZ,
522 21620426 to QQ), Huang Zhendong Research Fund for Traditional Chinese Medicine
523 of Jinan University (201911 to JC), and grant-in-Aid for Scientific Research (B) of
524 Japan Society for the Promotion of Science (21H02846 to KH).

525

526 AUTHOR CONTRIBUTIONS

527 JZ, QQ and KH conceived of the project, designed the experiments, analyzed the data,
528 and wrote the manuscript. QC, SL and WY designed and performed most of the
529 experiments and analyzed the data. YQ performed western blot analysis of postmortem
530 brain samples. NW assisted in behavior tests. SM provided postmortem brain samples
531 from control and DLB patients. ZZ provided pEGFP- -Syn, mGST- -Syn plasmid and
532 A53T mice. JH and JC assisted with data analysis and interpretation and critically read
533 the manuscript.

534

535 DECLARATION OF INTERESTS

536 The authors declare that they have no conflicts of interest.

537

538 KEYWORDS

539 Alpha-Synuclein; BDNF; Oligonucleotide; Transcription; Parkinson's disease

540

541 REFERENCE

- 542 1. Kang, SS, Zhang, Z, Liu, X, Manfredsson, FP, He, L, Iuvone, PM, Cao, XB,
543 Sun, Y, Jin, LJ, Ye KQ (2017). alpha-Synuclein binds and sequesters PIKE-L
544 into Lewy bodies, triggering dopaminergic cell death via AMPK
545 hyperactivation. *Proceedings of the National Academy of Sciences of the United*
546 *States of America* **114**: 1183-1188.
- 547 2. Ascherio, A, and Schwarzschild, MA (2016). The epidemiology of Parkinson's
548 disease: risk factors and prevention. *Lancet Neurol* **15**: 1257-1272.
- 549 3. Dauer, W, and Przedborski, S (2003). Parkinson's disease: mechanisms and
550 models. *Neuron* **39**: 889-909.
- 551 4. Yang, J, Luo, S, Zhang, J, Yu, T, Fu, Z, Zheng, Y, Xu, X, Liu CY, Fan MX,
552 Zhang, ZT (2020). Exosome-mediated delivery of antisense oligonucleotides
553 targeting alpha-synuclein ameliorates the pathology in a mouse model of
554 Parkinson's disease. *Neurobiol Dis* **148**: 105218.
- 555 5. Volpicelli-Daley, LA, Luk, KC, Patel, TP, Tanik, SA, Riddle, DM, Stieber, A,
556 Meaney DF, Trojanowski JQ, Lee VMY (2011). Exogenous α -synuclein fibrils
557 induce Lewy body pathology leading to synaptic dysfunction and neuron death.
558 *Neuron* **72**: 57-71.
- 559 6. Ellis, CE, Schwartzberg, PL, Grider, TL, Fink, DW, and Nussbaum, RL (2001).
560 alpha-Synuclein is phosphorylated by members of the Src family of protein-
561 tyrosine kinases. *J Biol Chem* **276**: 3879-3884.
- 562 7. Okochi, M, Walter, J, Koyama, A, Nakajo, S, Baba, M, Iwatsubo, T, Meijer, L,
563 Kahle, PJ, and Haass, C (2000). Constitutive phosphorylation of the Parkinson's
564 disease associated alpha-synuclein. *J Biol Chem* **275**: 390-397.
- 565 8. Jiang, P, Gan, M, Ebrahim, AS, Castanedes-Casey, M, Dickson, DW, and Yen,
566 SH (2013). Adenosine monophosphate-activated protein kinase overactivation
567 leads to accumulation of alpha-synuclein oligomers and decrease of neurites.
568 *Neurobiol Aging* **34**: 1504-1515.
- 569 9. Lashuel, HA, Overk, CR, Oueslati, A, and Masliah, E (2013). The many faces
570 of α -synuclein: from structure and toxicity to therapeutic target. *Nature reviews*
571 *Neuroscience* **14**: 38-48.
- 572 10. Toffoli, M, Vieira, SRL, and Schapira, AHV (2020). Genetic causes of PD: A
573 pathway to disease modification. *Neuropharmacology* **170**: 108022.

- 574 11. Zhang, J, Li, X, and Li, JD (2019). The Roles of Post-translational
575 Modifications on α -Synuclein in the Pathogenesis of Parkinson's Diseases.
576 *Frontiers in neuroscience* **13**: 381.
- 577 12. Kang, SS, Zhang, Z, Liu, X, Manfredsson, FP, Benskey, MJ, Cao, X, Xu, J, Sun,
578 Y, and Ye, KQ. (2017). TrkB neurotrophic activities are blocked by alpha-
579 synuclein, triggering dopaminergic cell death in Parkinson's disease.
580 *Proceedings of the National Academy of Sciences of the United States of*
581 *America* **114**: 10773-10778.
- 582 13. Huang, EJ, and Reichardt, LF (2003). Trk receptors: Roles in neuronal signal
583 transduction. *Annu Rev Biochem* **72**: 609-642.
- 584 14. Mizui, T, Ishikawa, Y, Kumanogoh, H, and Kojima, M (2016). Neurobiological
585 actions by three distinct subtypes of brain-derived neurotrophic factor: Multi-
586 ligand model of growth factor signaling. *Pharmacol Res* **105**: 93-98.
- 587 15. Zhang, JC, Yao, W, and Hashimoto, K (2016). Brain-derived Neurotrophic
588 Factor (BDNF)-TrkB Signaling in Inflammation-related Depression and
589 Potential Therapeutic Targets. *Curr Neuropharmacol* **14**: 721-731.
- 590 16. Seroogy, KB, Lundgren, KH, Tran, TM, Guthrie, KM, Isackson, PJ, and Gall,
591 CM (1994). Dopaminergic neurons in rat ventral midbrain express brain-
592 derived neurotrophic factor and neurotrophin-3 mRNAs. *J Comp Neurol* **342**:
593 321-334.
- 594 17. Baydyuk, M, and Xu, B (2014). BDNF signaling and survival of striatal neurons.
595 *Front Cell Neurosci* **8**: 254.
- 596 18. Howells, DW, Porritt, MJ, Wong, JY, Batchelor, PE, Kalnins, R, Hughes, AJ,
597 and Donnan GA. (2000). Reduced BDNF mRNA expression in the Parkinson's
598 disease substantia nigra. *Exp Neurol* **166**: 127-135.
- 599 19. Bambah-Mukku, D, Travaglia, A, Chen, DY, Pollonini, G, and Alberini, CM.
600 (2014). A positive autoregulatory BDNF feedback loop via C/EBP β mediates
601 hippocampal memory consolidation. *The Journal of neuroscience : the official*
602 *journal of the Society for Neuroscience* **34**: 12547-12559.
- 603 20. Martinowich, K, Hattori, D, Wu, H, Fouse, S, He, F, Hu, Y, and Fan, GP, and
604 Sun Y. (2003). DNA methylation-related chromatin remodeling in activity-
605 dependent BDNF gene regulation. *Science* **302**: 890-893.
- 606 21. Yuan, Y, Sun, J, Zhao, M, Hu, J, Wang, X, Du, G, and Chen, N. (2010).

- 607 Overexpression of alpha-synuclein down-regulates BDNF expression. *Cellular*
608 *and molecular neurobiology* **30**: 939-946.
- 609 22. Nishina, K, Piao, W, Yoshida-Tanaka, K, Sujino, Y, Nishina, T, Yamamoto, T,
610 Nitta, K, Yoshioka, K, Kuwahara, H, Yasuhara, H, *et al.* (2015). DNA/RNA
611 heteroduplex oligonucleotide for highly efficient gene silencing. *Nature*
612 *communications* **6**: 7969.
- 613 23. Yoshioka, K, Kunieda, T, Asami, Y, Guo, H, Miyata, H, Yoshida-Tanaka, K,
614 Sujino, Y, Piao, WY, Kuwahara, H, and Nishina, K, *et al.* (2019). Highly
615 efficient silencing of microRNA by heteroduplex oligonucleotides. *Nucleic*
616 *Acids Res* **47**: 7321-7332.
- 617 24. Asada, K, Sakaue, F, Nagata, T, Zhang, JC, Yoshida-Tanaka, K, Abe, A, Nawa
618 M, Nishina, K, and Tokota, T. (2021). Short DNA/RNA heteroduplex
619 oligonucleotide interacting proteins are key regulators of target gene silencing.
620 *Nucleic Acids Res* **49**: 4864-4876.
- 621 25. Ren, Q, Ma, M, Yang, J, Nonaka, R, Yamaguchi, A, Ishikawa, KI, Kobayashi K,
622 Murayama S, Hwang SH, *et al.* (2018). Soluble epoxide hydrolase plays a key
623 role in the pathogenesis of Parkinson's disease. *Proceedings of the National*
624 *Academy of Sciences of the United States of America* **115**: E5815-E5823.
- 625 26. Dickson, DW (2018). Neuropathology of Parkinson disease. *Parkinsonism*
626 *Relat Disord* **46 Suppl 1**: S30-S33.
- 627 27. Luo, S, Kang, SS, Wang, ZH, Liu, X, Day, JX, Wu, Z, Peng, J, Xiang, DX,
628 Springer, W, and Ye, KQ. (2019). Akt Phosphorylates NQO1 and Triggers its
629 Degradation, Abolishing Its Antioxidative Activities in Parkinson's Disease.
630 *The Journal of neuroscience : the official journal of the Society for*
631 *Neuroscience* **39**: 7291-7305.
- 632 28. Fumagalli, F, Racagni, G, and Riva, MA (2006). Shedding light into the role of
633 BDNF in the pharmacotherapy of Parkinson's disease. *Pharmacogenomics J* **6**:
634 95-104.
- 635 29. Jin, W (2020). Regulation of BDNF-TrkB Signaling and Potential Therapeutic
636 Strategies for Parkinson's Disease. *J Clin Med* **9**.
- 637 30. Bathina, S, and Das, UN (2015). Brain-derived neurotrophic factor and its
638 clinical implications. *Arch Med Sci* **11**: 1164-1178.
- 639 31. Molina-Holgado, F, Doherty, P, and Williams, G (2008). Tandem repeat peptide

- 640 strategy for the design of neurotrophic factor mimetics. *CNS Neurol Disord*
641 *Drug Targets* **7**: 110-119.
- 642 32. Sun, M, Kong, LX, Wang, XD, Lu, XG, Gao, QS, and Geller, AI (2005).
643 Comparison of the capability of GDNF, BDNF, or both, to protect nigrostriatal
644 neurons in a rat model of Parkinson's disease. *Brain Research* **1052**: 119-129.
- 645 33. Devi, L, Raghavendran, V, Prabhu, BM, Avadhani, NG, and
646 Anandatheerthavarada, HK (2008). Mitochondrial import and accumulation of
647 alpha-synuclein impair complex I in human dopaminergic neuronal cultures and
648 Parkinson disease brain. *J Biol Chem* **283**: 9089-9100.
- 649 34. Conway, KA, Rochet, JC, Bieganski, RM, and Lansbury, PT (2001). Kinetic
650 stabilization of the alpha-synuclein protofibril by a dopamine-alpha-synuclein
651 adduct. *Science* **294**: 1346-1349.
- 652 35. Xu, J, Kao, SY, Lee, FJS, Song, WH, Jin, LW, and Yankner, BA (2002).
653 Dopamine-dependent neurotoxicity of alpha-synuclein: A mechanism for
654 selective neurodegeneration in Parkinson disease. *Nature medicine* **8**: 600-606.
- 655 36. Barcia, C, Fernandez Barreiro, A, Poza, M, and Herrero, MT (2003).
656 Parkinson's disease and inflammatory changes. *Neurotox Res* **5**: 411-418.
- 657 37. Halliday, GM, and Stevens, CH (2011). Glia: initiators and progressors of
658 pathology in Parkinson's disease. *Mov Disord* **26**: 6-17.
- 659 38. Taylor, JM, Main, BS, and Crack, PJ (2013). Neuroinflammation and oxidative
660 stress: co-conspirators in the pathology of Parkinson's disease. *Neurochem Int*
661 **62**: 803-819.
- 662 39. Costa, G, Frau, L, Wardas, J, Pinna, A, Plumitallo, A, and Morelli, M (2013).
663 MPTP-Induced Dopamine Neuron Degeneration and Glia Activation Is
664 Potentiated in MDMA-Pretreated Mice. *Movement Disord* **28**: 1957-1965.
- 665 40. Wi, R, Chung, YC, and Jin, BK (2020). Functional Crosstalk between CB and
666 TRPV1 Receptors Protects Nigrostriatal Dopaminergic Neurons in the MPTP
667 Model of Parkinson's Disease. *J Immunol Res* **2020**.
- 668 41. Shahmoradian, SH, Lewis, AJ, Genoud, C, Hench, J, Moors, TE, Navarro, PP,
669 Castaño-Díez, D, Schweighauser, G, Graff-Meyer, A, and Goldie, KN, *et al.*
670 (2019). Lewy pathology in Parkinson's disease consists of crowded organelles
671 and lipid membranes. *Nat Neurosci* **22**: 1099-1109.
- 672 42. Luk, KC, Kehm, V, Carroll, J, Zhang, B, O'Brien, P, Trojanowski, JQ, and Lee

- 673 VMY. (2012). Pathological alpha-synuclein transmission initiates Parkinson-
674 like neurodegeneration in nontransgenic mice. *Science* **338**: 949-953.
- 675 43. Anderson, JP, Walker, DE, Goldstein, JM, de Laat, R, Banducci, K, Caccavello,
676 RJ, Barbour, R, Huang, JP, Kling, K, and Lee, M, *et al.* (2006). Phosphorylation
677 of Ser-129 is the dominant pathological modification of alpha-synuclein in
678 familial and sporadic Lewy body disease. *J Biol Chem* **281**: 29739-29752.
- 679 44. Arawaka, S, Sato, H, Sasaki, A, Koyama, S, and Kato, T (2017). Mechanisms
680 underlying extensive Ser129-phosphorylation in alpha-synuclein aggregates.
681 *Acta Neuropathol Commun* **5**: 48.
- 682 45. Karampetsou, M, Ardah, MT, Semitekoulou, M, Polissidis, A, Samiotaki, M,
683 Kalomoiri, M, Majbour, N, Xanthou, G, Ei-Agnaf, OMA, Vekrellis, K. (2017).
684 Phosphorylated exogenous alpha-synuclein fibrils exacerbate pathology and
685 induce neuronal dysfunction in mice. *Sci Rep* **7**: 16533.
- 686 46. Cabin, DE, Shimazu, K, Murphy, D, Cole, NB, Gottschalk, W, McIlwain, KL,
687 Orrison, B, Chen, A, Ellis, C, and paylor, R, *et al.* (2002). Synaptic vesicle
688 depletion correlates with attenuated synaptic responses to prolonged repetitive
689 stimulation in mice lacking alpha-synuclein. *The Journal of neuroscience : the*
690 *official journal of the Society for Neuroscience* **22**: 8797-8807.
- 691 47. Ekstrand, MI, Terzioglu, M, Galter, D, Zhu, S, Hofstetter, C, Lindqvist, E,
692 Thams S, Bergstrand A, Hansson FS, Trifunovic A, *et al.* (2007). Progressive
693 parkinsonism in mice with respiratory-chain-deficient dopamine neurons.
694 *Proceedings of the National Academy of Sciences of the United States of*
695 *America* **104**: 1325-1330.
- 696 48. Frahm, S, Melis, V, Horsley, D, Rickard, JE, Riedel, G, Fadda, P, Scherma, M,
697 Harrington, CR, Wischik, CM, and Theuring, F, *et al.* (2018). Alpha-Synuclein
698 transgenic mice, h-alpha-SynL62, display alpha-Syn aggregation and a
699 dopaminergic phenotype reminiscent of Parkinson's disease. *Behav Brain Res*
700 **339**: 153-168.
- 701 49. Sanders, DW, Kaufman, SK, DeVos, SL, Sharma, AM, Mirbaha, H, Li, A,
702 Barker, SJ, Foley, AC, Thorpe, JR, and Serpell, LC, *et al.* (2014). Distinct tau
703 prion strains propagate in cells and mice and define different tauopathies.
704 *Neuron* **82**: 1271-1288.
- 705 50. Kang, SS, Ahn, EH, Zhang, ZT, Liu, X, Manfredsson, FP, Sandoval, IM, Dhakal,

- 706 S, Iuvone, PM, Cao, XB, Ye, KQ. (2018). alpha-Synuclein stimulation of
707 monoamine oxidase-B and legumain protease mediates the pathology of
708 Parkinson's disease. *Embo J* **37**: e98878.
- 709 51. Volpicelli-Daley, LA, Luk, KC, and Lee, VM (2014). Addition of exogenous -
710 synuclein preformed fibrils to primary neuronal cultures to seed recruitment of
711 endogenous -synuclein to Lewy body and Lewy neurite-like aggregates.
712 *Nature protocols* **9**: 2135-2146.
- 713 52. Kim, J, Lee, S, Choi, BR, Yang, H, Hwang, Y, Park, JH, LaFerla FM, Han JS,
714 and Lee KW, *et al.* (2017). Sulforaphane epigenetically enhances neuronal
715 BDNF expression and TrkB signaling pathways. *Mol Nutr Food Res* **61**(2).
- 716 53. Pruunsild, P, Sepp, M, Orav, E, Koppel, I, and Timmusk, T (2011). Identification
717 of cis-elements and transcription factors regulating neuronal activity-dependent
718 transcription of human BDNF gene. *The Journal of neuroscience : the official*
719 *journal of the Society for Neuroscience* **31**: 3295-3308.
- 720 54. Saito, Y, Kawashima, A, Ruberu, NN, Fujiwara, H, Koyama, S, Sawabe, M,
721 Arai, M, Nagura, H, Yamanouchi, H, and Hasegawa, M, *et al.* (2003).
722 Accumulation of phosphorylated alpha-synuclein in aging human brain. *J*
723 *Neuropathol Exp Neurol* **62**: 644-654.
724
725

726 **Figures legends**727 **Figure 1. Overexpression α -Syn inhibits BDNF expression**

728 **A:** Western blot assay for p-CREB, CREB, BDNF, and MeCP2 in SH-SY5Y cells 24
 729 hours after GFP- α -Syn transfection (mean \pm SEM, n = 4 per group, Student's *t*-test, **p*
 730 < 0.05, ***p* < 0.01, and ****p* < 0.001). **B:** Protein expression of p-CREB, CREB, BDNF,
 731 and MeCP2 in the SNc of human AAV- α -Syn-treated mice (mean \pm SEM, n = 6 per
 732 group, Student's *t*-test, **p* < 0.05, ***p* < 0.01, and ****p* < 0.001). **C:** Protein expression
 733 of p-CREB, CREB, BDNF, and MeCP2 in the striatum from DLB patients and controls
 734 (mean \pm SEM, n = 10 per group, Student's *t*-test, **p* < 0.05, ***p* < 0.01, and ****p* <
 735 0.001). There was a positive correlation between BDNF levels and the ratio of
 736 phosphorylated CREB/CREB in DLB patients (n = 10). Furthermore, there was a
 737 negative correlation between BDNF levels and MeCP2 levels in DLB patients (n = 10).

738

739 **Figure 2. α -Syn-HDO activates BDNF transcription**

740 **A:** Schematic illustration of the construction of α -Syn-HDO. **B:** The internalization of
 741 FAM- α -Syn-HDO visualized by microscopy at 0 minutes, 30 minutes, and 1 hour
 742 following transfection of FAM- α -Syn-HDO (400 nM), Scale bar = 50 μ m. **C:** Western
 743 blot analysis of α -Syn, p-CREB, CREB, MeCP2, and BDNF in SH-SY5Y cells treated
 744 with various dosages of α -Syn-HDO (mean \pm SEM, n = 4 per group, one-way ANOVA,
 745 **p* < 0.05 and ***p* < 0.01). **D:** Luciferase assay for BDNF IV promoters. BDNF exon
 746 IV luciferase promoters and/or α -Syn-HDO were transfected into HEK293T cells.
 747 (mean \pm SEM, n = 4 per group, one-way ANOVA, ****p* < 0.001). **E:** BDNF exon IV
 748 luciferase promoter and α -Syn-HDO, siRNA-CREB plasmids, or mutation (Mut)
 749 plasmids were cotransfected into HEK293T cells (mean \pm SEM, n = 4 per group, one-
 750 way ANOVA, ***p* < 0.01 and ****p* < 0.001). **F:** CHIP-PCR assays demonstrated that
 751 p-CREB specifically binds to genomic DNA of BDNF exon IV promoter binding
 752 motifs. p-CREB protein-DNA crosslinking samples were obtained from SH-SY5Y
 753 cells treated with α -Syn-HDO or vehicle via coimmunoprecipitation with an anti-p-
 754 CREB antibody. PCR was performed with primers targeting the BDNF exon IV
 755 promoter. An anti-histone H3 antibody coupled with GAPDH primers was used as the
 756 positive control (mean \pm SEM, n = 4 per group, Student's *t*-test, **p* < 0.05). **G:** qPCR

757 assay for BDNF in SH-SY5Y cells treated with α -Syn-HDO (mean \pm SEM, n = 5 per
758 group, Student's *t*-test, **p* < 0.05).

759

760 **Figure 3. α -Syn-HDO attenuates BDNF downregulation in α -Syn-treated SH-**
761 **SY5Y cells**

762 **A:** Western blot assay for p-CREB, CREB, BDNF, and MeCP2 in GFP- α -Syn-
763 transfected SH-SY5Y cells treated with α -Syn-HDO for 24 hours (mean \pm SEM, n = 5
764 per group, one-way ANOVA, **p* < 0.05 and ***p* < 0.01). **B:** Immunofluorescence
765 staining for p-CREB and MeCP2 in GST- α -Syn-transfected SH-SY5Y cells treated
766 with α -Syn-HDO for 24 hours. Scale bar = 50 μ m.

767

768 **Figure 4. α -Syn-HDO attenuates dopaminergic neuron degeneration in AAV9-**
769 **hSyn-human SNCA-treated mice**

770 **A:** Schedule of treatment and graphical illustration of human AAV- α -Syn injection. **B:**
771 Graphical illustration of the intracerebroventricular injection site. **C:** Results of the
772 rotarod test (mean \pm SEM, n = 10–12 per group, one-way ANOVA, **p* < 0.05 and ***p*
773 < 0.01). **D:** Immunofluorescence staining for TH in the SNc. Quantification analysis of
774 TH (mean \pm SEM, n = 5 per group, one-way ANOVA, ***p* < 0.01 and ****p* < 0.001).
775 Scale bar = 50 μ m. **E:** Western blot assay for TH and α -Syn in the SNc (mean \pm SEM,
776 n = 5 per group, one-way ANOVA, **p* < 0.05, ***p* < 0.01 and ****p* < 0.001). **F:** ChIP-
777 PCR assays for p-CREB and BDNF exon IV promoter in the SNc (mean \pm SEM, n = 5
778 per group, one-way ANOVA, **p* < 0.05, ***p* < 0.01, and ****p* < 0.001). **G:** Western
779 blot assay for p-CREB/CREB, BDNF, and MeCP2 in the SNc (mean \pm SEM, n = 5 per
780 group, one-way ANOVA, **p* < 0.05, ***p* < 0.01, and ****p* < 0.001).

781

782 **Figure 5. α -Syn-HDO attenuates dopaminergic neuron degeneration in MPTP-**
783 **treated A53T mice**

784 **A:** Schedule of treatment. **B:** Results of the rotarod test (mean \pm SEM, n = 10–12 per
785 group, one-way ANOVA, $*p < 0.05$ and $**p < 0.01$). **C:** Immunofluorescence staining
786 for TH in the SNc. Quantification analysis of TH (mean \pm SEM, n = 5 per group, one-
787 way ANOVA, $**p < 0.01$ and $***p < 0.001$). Scale bar = 50 μ m. **D:** Western blot assay
788 for TH and α -Syn in the SNc (mean \pm SEM, n = 5 per group, one-way ANOVA, $*p <$
789 0.05 , $**p < 0.01$, and $***p < 0.001$). **E:** ChIP-PCR assays for p-CREB and BDNF exon
790 IV promoter in the SNc (mean \pm SEM, n = 5 per group, one-way ANOVA, $*p < 0.05$,
791 $**p < 0.01$ and $***p < 0.001$). **F:** Western blot assay for p-CREB/CREB, BDNF, and
792 MeCP2 in the SNc (mean \pm SEM, n = 5 per group, one-way ANOVA, $*p < 0.05$, $**p$
793 < 0.01 , and $***p < 0.001$).

794

795 **Figure 6. α -Syn-HDO prevents α -Syn-induced PD pathology**

796 **A:** Immunofluorescence staining for TH and p- α -Syn in the SNc. Scale bar = 50 μ m. **B:**
797 The schedule of treatment and the rotarod test results (mean \pm SEM, n = 11 or 12 per
798 group, one-way ANOVA, $**p < 0.01$ and $***p < 0.001$). **C:** Immunofluorescence
799 staining for TH in the SNc. Quantification analysis of TH (mean \pm SEM, n = 5 per
800 group, one-way ANOVA, $*p < 0.05$ and $**p < 0.01$). Scale bar = 50 μ m. **D:** Western
801 blot assay for TH, p- α -Syn, and α -Syn in the SNc (mean \pm SEM, n = 5 per group, one-
802 way ANOVA, $*p < 0.05$ and $**p < 0.01$). **E:** ChIP-PCR assays for p-CREB and BDNF
803 exon IV promoter in the SNc (mean \pm SEM, n = 5 per group, one-way ANOVA, $*p <$
804 0.05 , $**p < 0.01$ and $***p < 0.001$). **F:** Western blot assay for p-CREB/CREB, BDNF,
805 and MeCP2 in the SNc (mean \pm SEM, n = 5 per group, one-way ANOVA, $*p < 0.05$,
806 $**p < 0.01$, and $***p < 0.001$).

Figure 1**A**

Journal Pre-proof

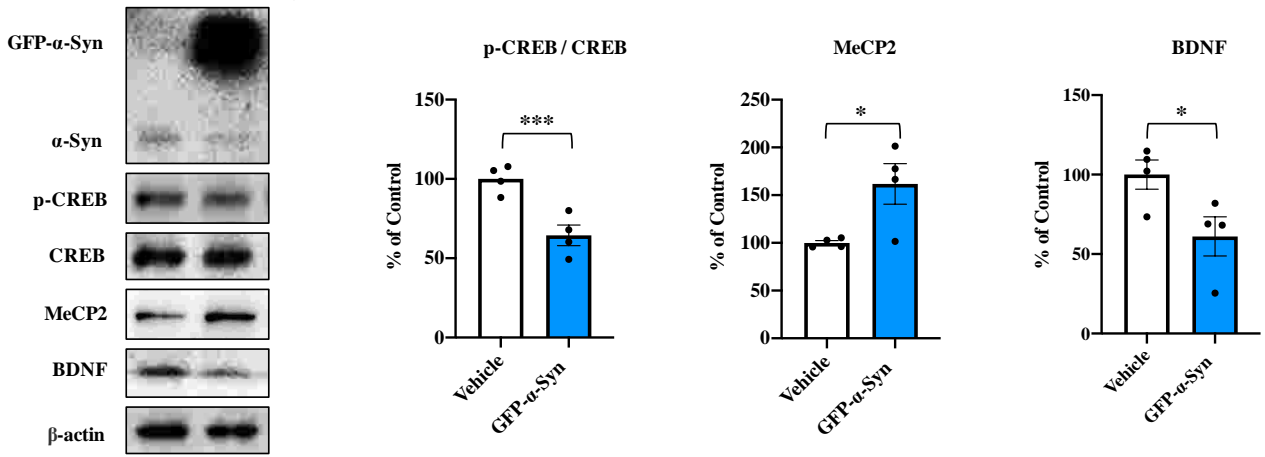
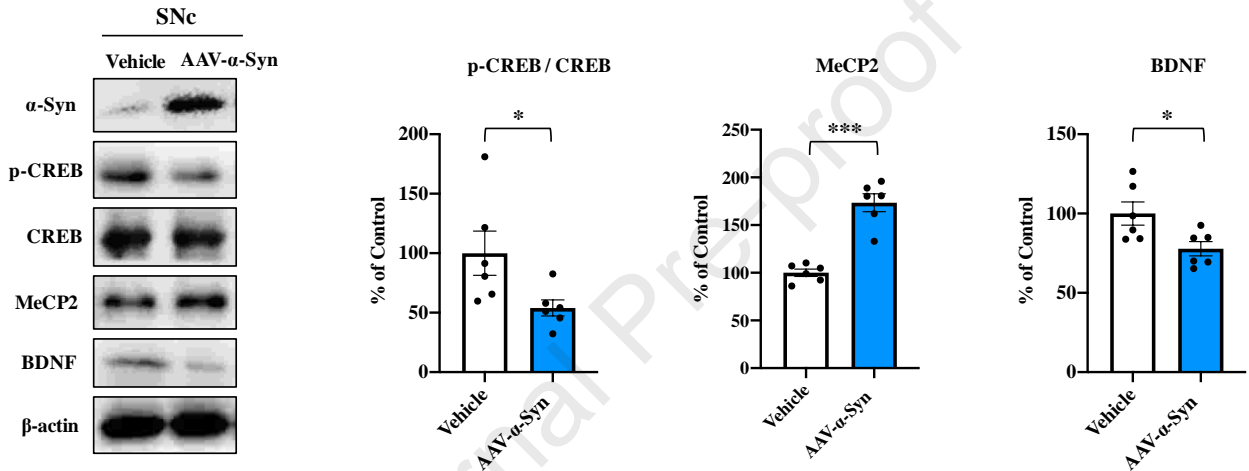
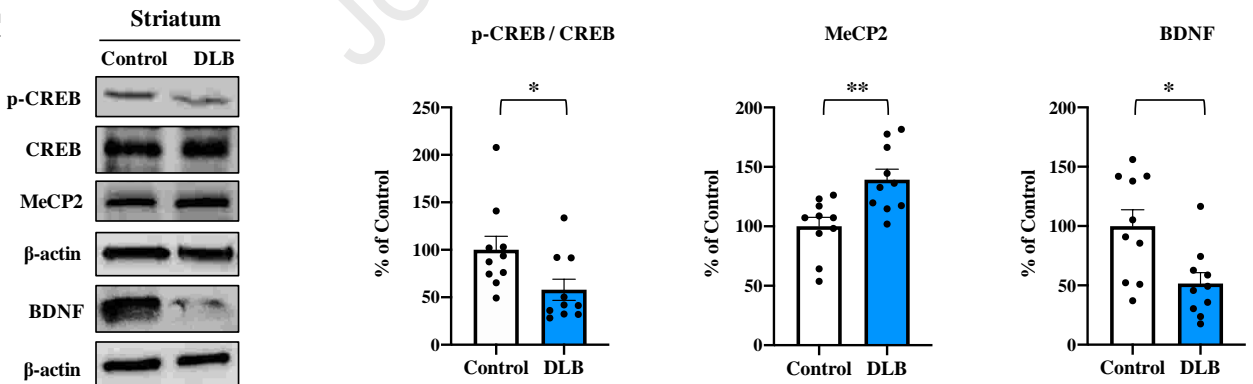
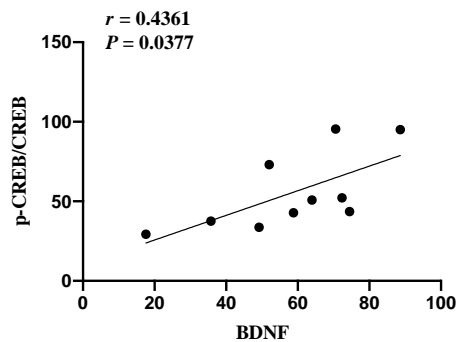
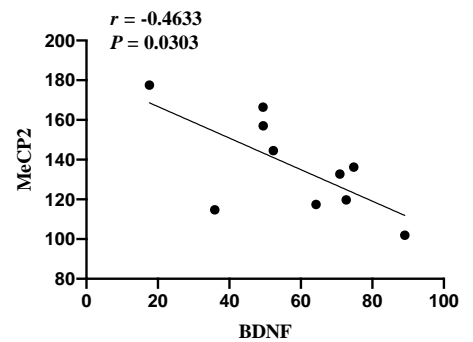
**B****C****BDNF = f(pCREB/CREB)****BDNF = f(MeCP2)**

Figure 2

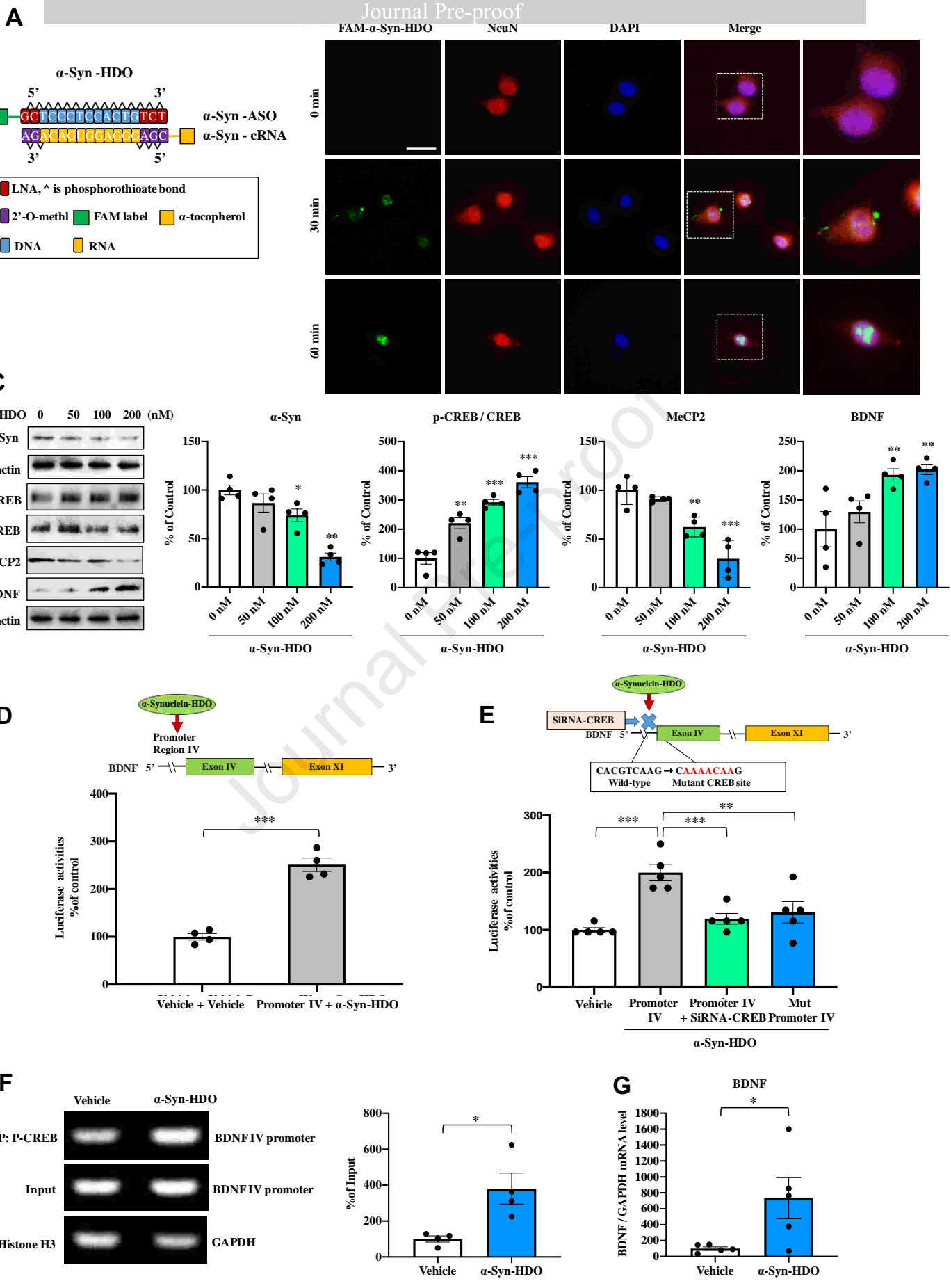
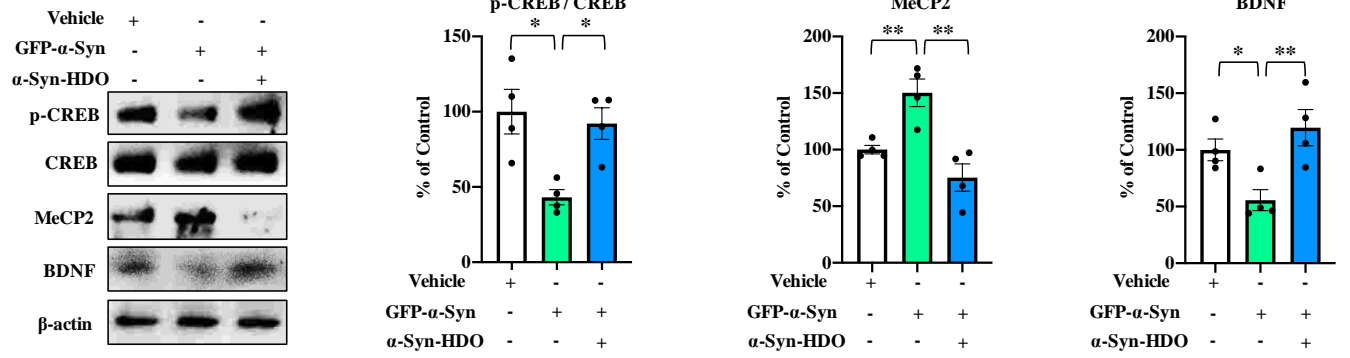


Figure 3

A



B

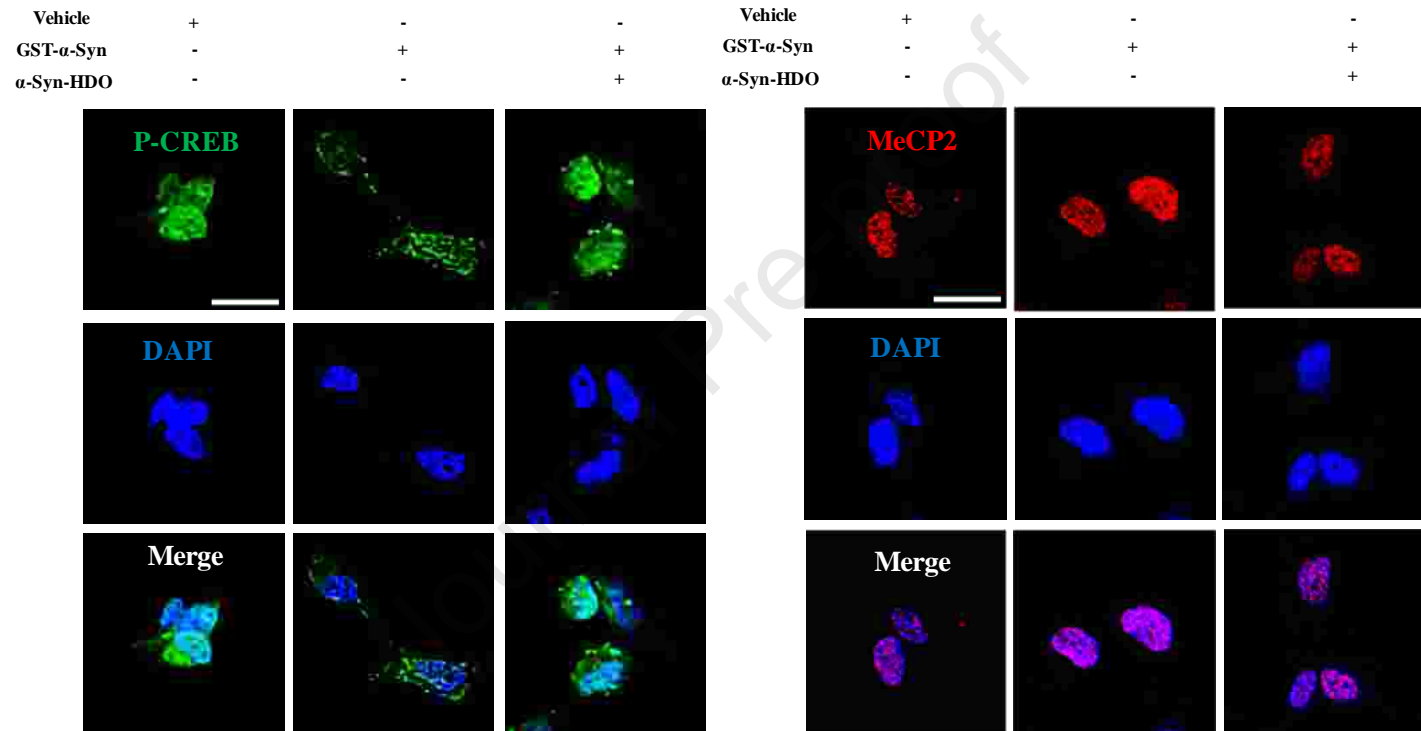
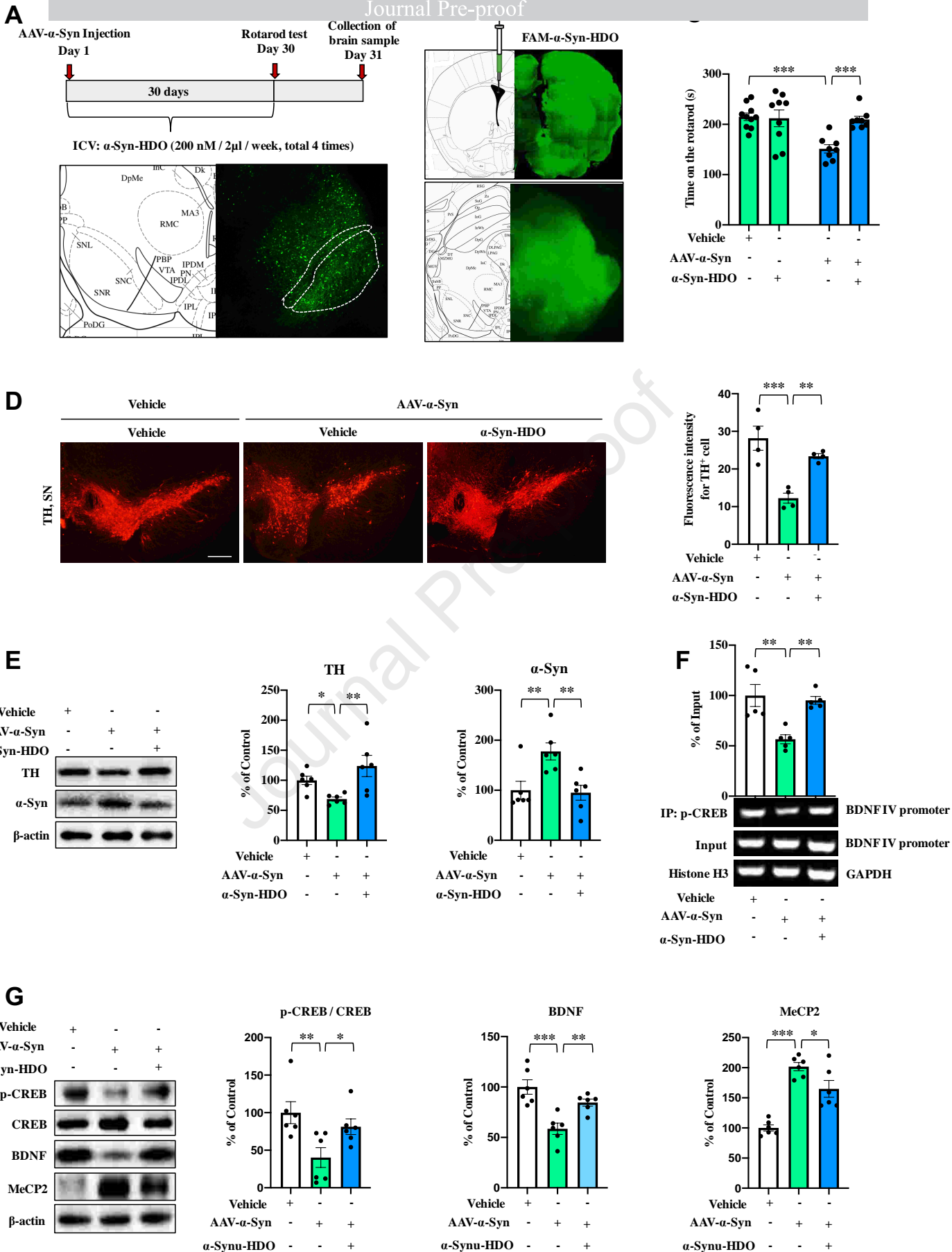
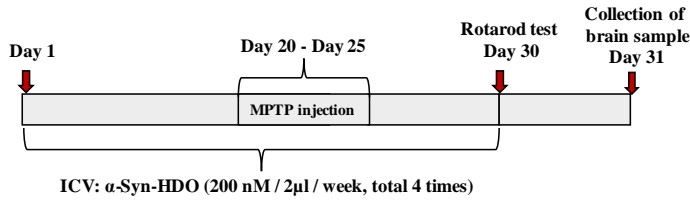


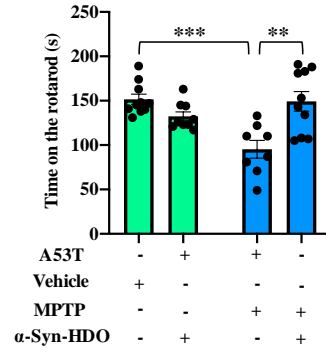
Figure 4



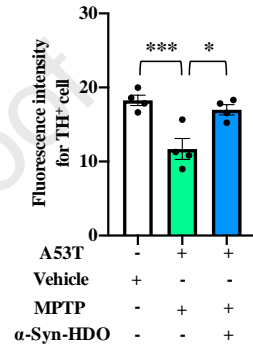
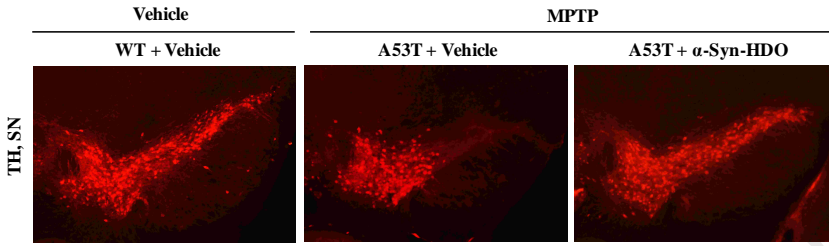
A



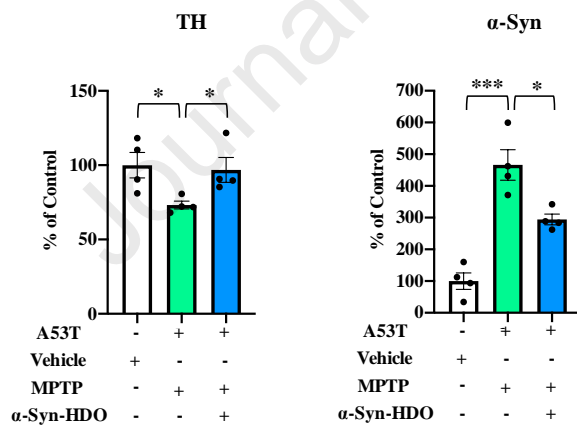
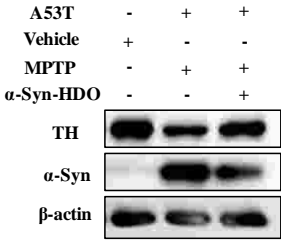
B



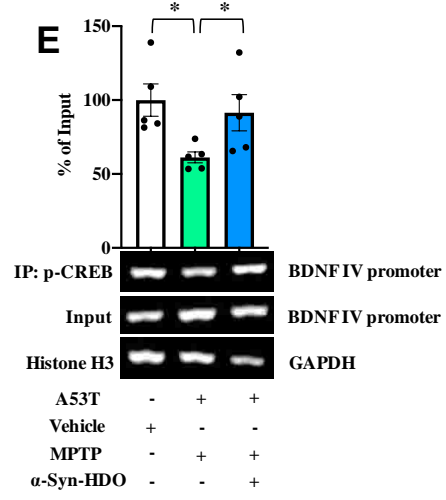
C



D



E



F

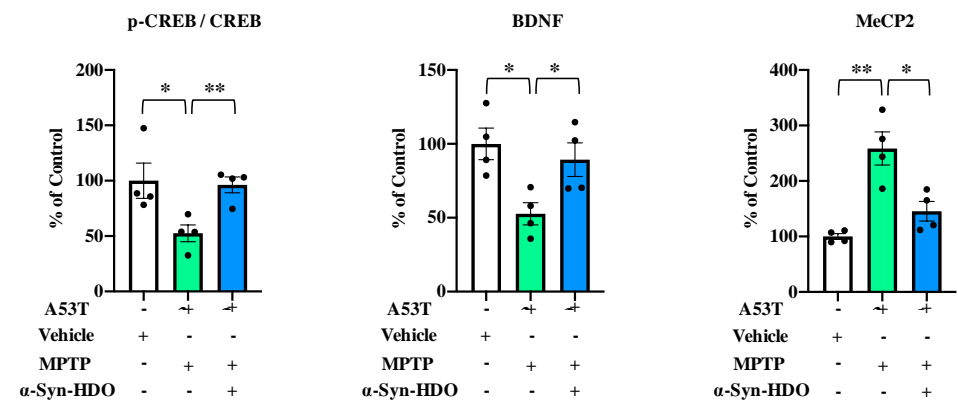
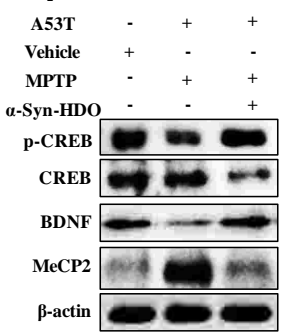
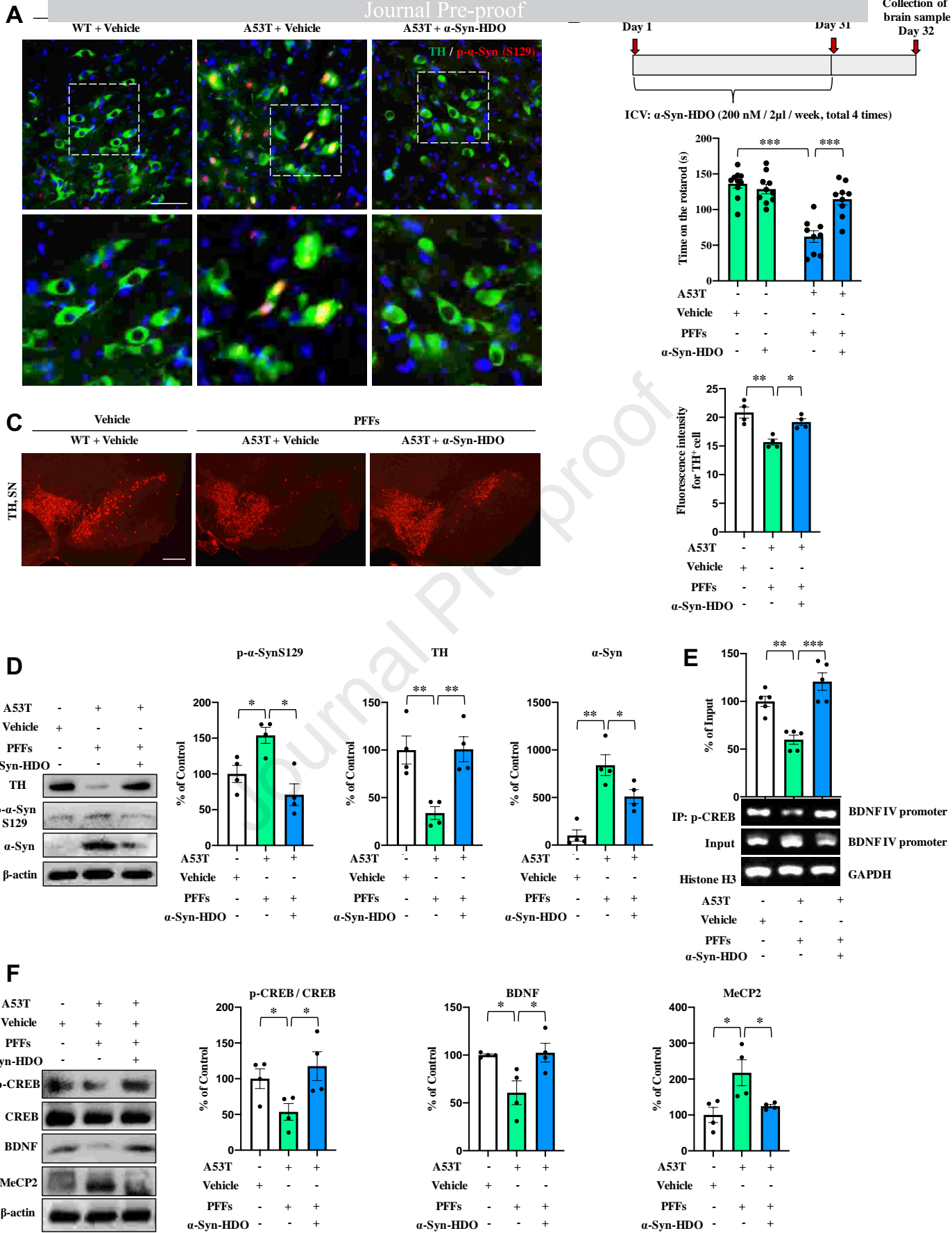


Figure 6



Abnormal α -Syn expression induces dopaminergic neuron degeneration via inhibition of BDNF transcription. The novel nucleic acid agent α -Syn-HDO can attenuate dopaminergic neurons degeneration in PD mouse models via activation of BDNF transcription.

Journal Pre-proof